Post-print of: Bekasiewicz A., Kozieł S.: EM-driven topology evolution for bandwidth enhancement of hybrid quadrature patch couplers. 2018 22nd International Microwave and Radar Conference (MIKON). DOI: 10.23919/MIKON.2018.8405169

EM-Driven Topology Evolution for Bandwidth Enhancement of Hybrid Quadrature Patch Couplers

Adrian Bekasiewicz[1]
[1] Faculty of Electronics, Telecommunications and Inf.
Gdansk University of Technology
Gdansk, Poland
bekasiewicz@ru.is

Slawomir Koziel[2]
[2] Engineering Optimization & Modeling Center
Reykjavik University
Reykjavik, Iceland
koziel@ru.is

***Abstract*—A broad operational bandwidth is one of the key performance figures of hybrid patch couplers. Due to the lack of systematic design procedures, bandwidth enhancement is normally obtained through manual modifications of the structure geometry. In this work, an optimization-based topology evolution for EM-driven design of patch couplers with enhanced bandwidth has been proposed. The method exploits a novel spline-based EM model where the spline control points (also referred to as knots) are defined in a cylindrical coordinate system. The model has been optimized in an unattended manner using a gradient-based algorithm embedded in a trust-region framework. Two design cases with 13 and 21 design parameters have been considered. The optimized structures are characterized by symmetrical bandwidth (defined for the maximum of 0.5 dB imbalance between S_{21} and S_{31}) of 23.4% and 31.6%, respectively. The obtained coupler topologies have been favorably compared with state-of-the-art patch broadband couplers reported in the literature.**

Keywords—Patch coupler; hybrid coupler; topology evolution; EM-driven design; bandwidth enhancement.

I. INTRODUCTION

Hybrid quadrature couplers realized in microstrip technology are vital components of many microwave devices including Butler matrices, power dividers, baluns, balanced mixers and others [1], [2]. At the same time, stringent requirements concerning center frequency and operational bandwidth are often imposed on modern communication systems, which may be difficult to meet using conventional branch-line couplers (BLCs). These problems can be partially addressed using patch couplers (PCs). Owing to simple topology—their conventional realizations are based on rectangular, circular and elliptical topologies [4]—and strong mechanical structure, PCs are easy to manufacture. Moreover, a relatively large size makes them suitable for high-frequency applications (especially from the fabrication point of view) [3]. Also, operational bandwidth of PCs is broader than for the BLC structures.

Advantages of patch couplers over conventional BLC circuits stimulate the research on increasing their usefulness for modern systems. In particular, PC structures are miniaturized to make them suitable for low-frequency applications [5], [6]. On the other hand, PCs are being implemented in substrate integrated waveguide (SIW) technology to extend their operational range to millimeter-waves [6]. Improved-performance structures have also gained significant attention. In [4], a method for design of PCs with arbitrarily selected coupling has been proposed. In [3], varactor-loaded ground plane slots have been incorporated to reconfigure port arrangement and allow for changing its coupling coefficient. Also, dual-band patch couplers based on stub-loaded topology have been proposed in [1]. Because broadband operation is one of the most important performance requirements of PCs, it is not surprising that circuits with enhanced bandwidth have also been considered in literature [4]-[6]. Broadband operation is normally obtained using various modifications of the patch (e.g., inclusion of stubs and slots [2], [8]). Alternatively, bandwidth broadening can be achieved through ground plane modifications in the form of slots or various defected-ground structures [4], [5].

Typical design flow of bandwidth-enhanced PCs includes selection of the reference design and manual modifications of its topology. Geometrical changes are often followed by parameter sweeps (normally one variable at a time) [4], [6]. On one hand, this experience-driven trial-and-error-based method is laborious, because reliable evaluation of patch couplers with modified topologies can only be realized using CPU-intensive electromagnetic (EM) analysis. On the other hand, manual design approaches fail to yield truly optimum solutions. Another problem is that design of a broadband structure requires simultaneous handling of at least three performance figures, i.e., coupling, reflection, and isolation, which cannot be effectively handled using parameter sweeps. These challenges can be addressed by means of numerical optimization algorithms [5]. However, optimization is normally applied to tune geometrical dimensions of a preselected circuit topology. In order to achieve competitive designs of bandwidth-enhanced couplers, a fully automated framework capable of adjusting

both the structure topology and its geometry parameters is required.

In this work, a systematic approach for EM-driven topology evolution of bandwidth enhanced patch couplers has been presented. The method exploits a novel, spline-based, EM model of the patch coupler. In contrary to the models considered in the literature [9], [10], here, the spline control points (referred to as knots) are defined in a cylindrical coordinate system so that their angular distance w.r.t each other is equal. This arrangement is more natural for the considered coupler geometry. It also addresses the problem of producing infeasible designs in the course of the optimization process (due to overlap of knots [9]). The proposed PC is optimized using a gradient-based algorithm embedded in a trust-region framework. Two design cases with 13 and 21 parameters are considered. Symmetrical bandwidths of the optimized structures (defined for the maximum of 0.5 dB imbalance between S_{21} and S_{31}) are 23.4% and 31.6%, respectively. The obtained circuits have been favorably compared to state-of-the-art patch couplers available in the literature.

II. Methodology

In this section, topology evolution for EM-driven design of patch couplers with enhanced bandwidth is presented. More specifically, we formulate the design problem, discuss implementation of the universal spline-based EM model and describe a design optimization framework. Numerical results and comparisons of the structure with benchmark couplers from the literature are given in Section III.

A. Design Specifications and Problem Formulation

To obtain the best possible performance of a coupler, a rigorous numerical optimization of its parameters is required. The design problem is given as

$$\boldsymbol{x}^* = \arg\min_{\boldsymbol{x}} U(\boldsymbol{R}(\boldsymbol{x})) \tag{1}$$

where $\boldsymbol{R}(\boldsymbol{x})$ is a response of the EM model of the PC, $\boldsymbol{x}$ is a vector of design parameters, and U is a scalar objective function, whereas $\boldsymbol{x}^*$ is the optimum design to be found. Here, the following design requirements are considered (f_0 is the operating frequency):

- Maximization of $f_{ds.f}$ defined as a symmetric (w.r.t. f_0) part of the frequency range such that $|S_{21}(\boldsymbol{x}) - S_{31}(\boldsymbol{x})| \le$ 0.5 dB for all frequencies within this range;
- Maintaining $|S_{11}|$ and $|S_{41}|$ at f_0 below –30 dB: $S_m = \max(\min\{S_{11}(\boldsymbol{x}),S_{41}(\boldsymbol{x})\}) \le -30$ dB (defined at f_0);
- Maintaining power split error at f_0 below 0.2 dB: $d_{S0} = |S_{21}(\boldsymbol{x}) - S_{31}(\boldsymbol{x})| \le 0.2$ dB.

Here, S_{11}, S_{21}, S_{31}, and S_{41} denote reflection, transmission, coupling, and isolation, respectively. The objective function is defined as

$$U(\boldsymbol{R}(\boldsymbol{x})) = -2\min\left\{f_0 - \min\left(f_{d_s.f}(\boldsymbol{x})\right), \max\left(f_{d_s.f}(\boldsymbol{x})\right) - f_0\right\} + \beta_1 c_1^{\,2} + \beta_2 c_2^{\,2} \tag{2}$$

Small power-split error, as well as low reflection and isolation at f_0 are enforced using penalty functions $c_1 = \max\{(d_{s0}(\boldsymbol{x}) - 0.2)/0.2,0\}$ and $c_2 = \max\{(S_m(\boldsymbol{x}) + 30)/30,0\}$. The coefficients β_1 and β_2 are set to 20.

B. Universal Spline-Based EM Coupler Model

Consider a generic microstrip patch coupler topology shown in Fig. 1. The structure is implemented in CST Microwave Studio [11]. It consists of a spline-parameterized patch and four 50 ohm feed lines. The circuit (i.e., its two quarters; see Fig. 1) is represented using 51 variables $\boldsymbol{y} = [D\ r_1\ r_2\ \ldots\ r_K]^T$, where D defines maximum allowed distance from the model center (in a cylindrical coordinate system) and r_k, $k = 1, \ldots K$, are relative variables with respect to D. The angular distance between the control points is constant and equal to π/K radians. The absolute radial coordinate of the kth control point of the spline-based shape is $D{\cdot}r_k$. Utilization of cylindrical coordinate system allows us to avoid infeasible topologies resulting from overlapping of the control points (possible in the Cartesian system; see e.g., [9], [10]). It should be emphasized that due to a large number of knots, the EM model can approximate rectangle-based shapes with reasonable accuracy.

It is worth mentioning that, for the proposed structure, the number of input parameters $\boldsymbol{x} = [D\ q_1\ q_2\ \ldots\ q_N]^T$, $N \le K$, used for topology evolution can be easily adjusted. This is realized through curve fitting of the parameters q_n and subsequent approximation of the obtained curve using spline composed using r_k points. At least four knots per quarter of the structure are required to create a spline curve ($N = 8$).

C. Optimization Algorithm

The design problem defined in Section II.*A* is challenging. Moreover, the proposed coupler EM model may contain a large number of input parameters. Therefore, a robust method is required for successful optimization of the structure. Here, a gradient-based algorithm embedded in the trust-region framework is utilized. The considered algorithm generates a series of approximations $\boldsymbol{x}^{(i)}$, $i = 0, 1, \ldots$ to the solution $\boldsymbol{x}^*$ of the original problem (1) as

$$\boldsymbol{x}^{(i+1)} = \arg\min_{\boldsymbol{x}:\|\boldsymbol{x}-\boldsymbol{x}^{(i)}\|\le\delta^{(i)}} U\left(\boldsymbol{G}_s^{(i)}(\boldsymbol{x})\right) \tag{3}$$

The linear expansion model $\boldsymbol{G}_s^{(i)}$ is of the following form

$$\boldsymbol{G}_s^{(i)}(\boldsymbol{x}) = \boldsymbol{R}(\boldsymbol{x}^{(i)}) + \boldsymbol{J}(\boldsymbol{x}^{(i)})\cdot(\boldsymbol{x} - \boldsymbol{x}^{(i)}) \tag{4}$$

Here, $\boldsymbol{J}$ is a Jacobian of $\boldsymbol{R}$ obtained through finite differentiation as [12]

$$\boldsymbol{J}(\boldsymbol{x}^{(i)}) = \left[\frac{\boldsymbol{R}(\boldsymbol{x}^{(i)}+\boldsymbol{h}_1) - \boldsymbol{R}(\boldsymbol{x}^{(j)})}{h_1} \quad \cdots \quad \frac{\boldsymbol{R}(\boldsymbol{x}^{(i)}+\boldsymbol{h}_M) - \boldsymbol{R}(\boldsymbol{x}^{(i)})}{h_M}\right]^T \tag{5}$$

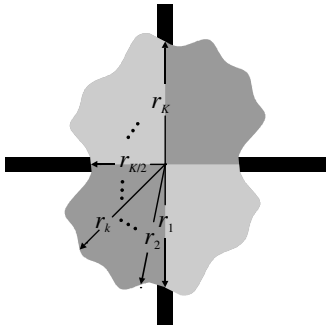

Fig. 1. Geometry of the considered universal spline-based EM model of a patch coupler. Different shades of gray denote symmetrical sections of the structure.

where $\boldsymbol{h} = [h_1 \ \ldots \ h_M]^T$, $M = N + 1$, in (5) is the perturbation vector, whereas $\boldsymbol{h}_n = [0 \ \ldots \ 0 \ h_m \ 0 \ \ldots \ 0]^T$, $m = 1, \ldots, M$. The trust region radius $\delta^{(i)}$ is updated using the standard rules based on a gain ratio ρ defined as

$$\rho = \frac{U(\boldsymbol{R}(\boldsymbol{x}^{(i+1)})) - U(\boldsymbol{R}(\boldsymbol{x}^{(i)}))}{U(\boldsymbol{G}^{(i)}(\boldsymbol{x}^{(i+1)})) - U(\boldsymbol{G}^{(i)}(\boldsymbol{x}^{(i)}))} \tag{6}$$

which is a ratio of the actual versus predicted improvement of the objective function (2). For $\rho > 0.9$ the radius is modified as $\delta^{(i+1)} = \max(2.5\|\boldsymbol{x}^{(i+1)} - \boldsymbol{x}^{(i)}\|, \delta^{(i)})$. When $\rho < 0.05$ it is reduced as $\delta^{(i+1)} = 0.25\|\boldsymbol{x}^{(i+1)} - \boldsymbol{x}^{(i)}\|$. The new design is only accepted if $\rho > 0$; otherwise it is rejected and the search is restarted from $\boldsymbol{x}^{(i)}$.The initial radius is $\delta^{(0)} = 1$. The computational cost of one algorithm iteration is $M + 1$ evaluations of the structure EM model. Extra simulations are required for unsuccessful iterations (i.e., with $\rho < 0$). More detailed discussion of the considered algorithm can be found e.g., in [12], [13].

III. Numerical Results

In this section, the bandwidth-enhancement-oriented design of the hybrid patch coupler based on the concept of topology evolution is performed. Comparison of the obtained designs with state-of-the-art couplers is also provided.

A. Initial Design

The initial design of the coupler $\boldsymbol{x}_0^{(0)} = [D \ q_1 \ q_2]^T$, where $q_2 = 1$, is based on the circular sector patch topology. Equal power-split has been obtained by maintaining ratio q_2/q_1 of around 1.3 [4]. Note that D is in mm, whereas q_k are unitless. The substrate is a 0.762 mm thick Arlon AR250D (ε_r = 2.5, tanδ = 0.0018). The center frequency is set to f_0 = 10 GHz. The initial radius of the patch (r = 5.25 mm) has been obtained from [13]

$$f_0 = \frac{184.118c}{2\pi r_{ef} \varepsilon_r^{0.5}} \tag{7}$$

where effective patch radius r_{ef} is given by

$$r_{ef} = 0.1r + \frac{0.1rh}{r+h}\left(\begin{array}{l} 0.376\cos\left(\varepsilon_r^{4.774} + 3.176\,h/r\right) \\ +\cos\left(1/\varepsilon_r + 0.01rh\right) - 0.389 \end{array}\right) \tag{8}$$

The obtained design parameter vector $\boldsymbol{x}_0^{(0)} = [6.82 \ 0.765 \ 1]^T$ (D = 1.3r) has been then optimized for minimum $|S_{11}|$ and $|S_{41}|$ while maintaining $d_{s0} < 0.2$ (all at the center frequency). The resulting design $\boldsymbol{x}_0^* = [6.57 \ 0.763 \ 1]^T$ is selected as a starting point for the evolution of the coupler topology. The geometry of the structure as well as its frequency characteristics at the initial and the optimized designs are shown in Fig. 2.

B. Topology Evolution

Two design cases with 13 (Case I) and 21 (Case II) variables are considered. The design bounds for the optimization process are: $\boldsymbol{l} = [3 \ 0.1 \ \ldots \ 0.1]^T$ and $\boldsymbol{u} = [10 \ 1 \ \ldots \ 1]^T$. The initial design for the first structure is $\boldsymbol{x}_\mathbf{I}^{(0)} = [5.01 \ 0.763 \ 0.763 \ 0.763 \ 0.763 \ 0.763 \ 0.763 \ 1 \ 1 \ 1 \ 1 \ 1 \ 1]^T$. The coupler has been optimized using the algorithm of Section II.*C*. The final design $\boldsymbol{x}_\mathbf{I}^*$=[7.4 0.8 0.7 0.61 0.56 0.75 0.76 1 0.9 0.77 0.9 0.98 0.99]^T, has been found after 9 iterations. The resulting 0.5-dB bandwidth of the optimized structure is 2.34 GHz, which is 11 percent broader compared to the initial design (2.1 GHz).

Next, the design $\boldsymbol{x}_\mathbf{I}^*$ has been used as a starting point for the Case II. The final parameter vector $\boldsymbol{x}_\mathbf{II}^*$ = [7.61 0.8 0.76 0.71 0.61 0.56 0.55 0.59 0.73 0.81 0.75 1 0.99 0.84 0.78 0.79 0.85 0.91 0.95 0.97 0.99]^T has been obtained after 10 algorithm iterations. The structure 0.5 dB bandwidth is 3.16 GHz, 51% and 35% broader compared to $\boldsymbol{x}_0^*$ and $\boldsymbol{x}_\mathbf{I}^*$, respectively. Topologies of the optimized couplers and their frequency characteristics are shown in Figs. 3 and 4, respectively. The obtained results clearly indicate a substantial bandwidth enhancement that can be achieved by increasing flexibility of the model (in terms of the number of degrees of freedom) along with automated evolution of its topology.

C. Comparisons

The designs obtained through evolution of the patch coupler topology have been compared to other state-of-the-art circuits in terms of bandwidth (BW). It should be noted that BW of structures from the literature is normally defined using 1-dB imbalance between $|S_{21}|$ and $|S_{31}|$. Moreover, BW symmetry around f_0 is rarely considered. Therefore, BW figures of the obtained couplers have been recalculated to 1-dB imbalance (without symmetry constraint). The obtained bandwidths are 34.1% and 45.2% for Case I and II, respectively.

Even though the proposed structures have not been optimized w.r.t. size, their footprints (expressed in guided wavelength) have been also included. The results shown in Table I indicate that the couplers obtained through topology evolution outperform circuits for which bandwidth-enhancement has been achieved by means of arbitrary modifications of the topology. At the same time, sizes of the proposed structures are competitive, whereas their simple and smooth topologies (which might not the case for bandwidth-enhanced couplers, see [5]) make them easy to manufacture.

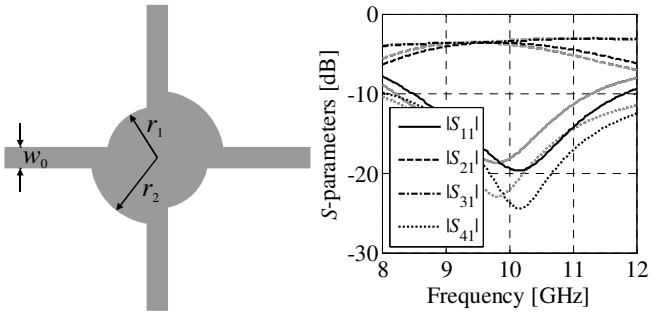

Fig. 2. Initial design of the coupler: (a) topology and (b) frequency characteristics before (gray) and after (black) optimization.

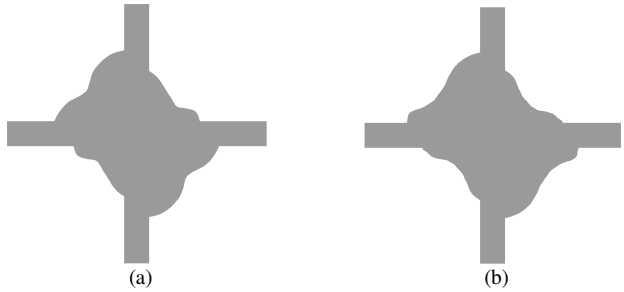

Fig. 3. Topologies of obtained patch couplers: (a) Case I and (b) Case II.

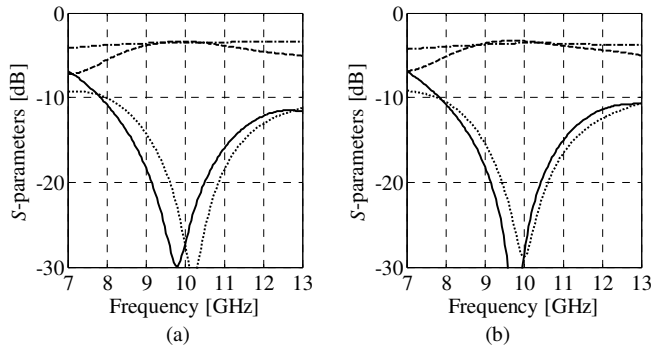

Fig. 4. $|S_{11}|$ (—),$|S_{21}|$ (– –), $|S_{31}|$ (–·), and $|S_{41}|$ (···) responses of optimized patch coupler topologies: (a) Case I and (b) Case II.

TABLE I PERFORMANCE COMPARISON WITH BENCHMARK COUPLERS

Coupler	f_0 [GHz]	BW [%]	BW [GHz]	Size [mm × mm]	Size [λ_g^2]
[7]	30	11.2	3.36	8.1 × 9.6	1.46
[2]	4.0	36.7	1.47	36.0 × 44.1	0.61
[5]	3.5	38.2	1.34	18.0 × 24.4	0.12
[4]	10	35.5	3.55	12.0 × 12.0	0.31
This work (Case I)	10	34.1	3.41	14.8 × 14.8	0.51
This work (Case II)	10	45.2	4.52	15.2 × 15.2	0.53

IV. CONCLUSION

In this work, a method for a systematic design of patch couplers with enhanced bandwidth based on topology evolution concept has been proposed. In the approach, a novel EM model of the coupler is used where the control points of the spline curves are defined in cylindrical coordinate system. The proposed model has been optimized for maximization of bandwidth (while ensuring low power split error, as well as low reflection and isolation at the center frequency of 10 GHz) using the gradient-based algorithm embedded in the trust-region framework. Optimizations have been performed for cases with 13 and 21 variables. The resulting symmetrical 0.5-dB imbalance bandwidths are 23.4% and 31.6% (34.1% and 45.2% for non-symmetrical 1-dB bandwidths), respectively. The obtained designs outperform other state-of-the-art couplers in terms of performance. Future work will focus on application of the proposed approach for automated design of planar antennas.

ACKNOWLEDGMENT

The authors would like to thank Dassault Systems, France, for making CST Microwave Studio available. This work was supported in part by the Icelandic Centre for Research (RANNIS) Grant 163299051, and by National Science Centre of Poland Grant 2015/17/B/ST6/01857.

REFERENCES

[1] S.Y. Zheng, S.H. Yeung, W.S. Chan, K.F. Man, S.H. Leung, and Q. Xue, "Dual-band rectangular patch hybrid coupler," *IEEE Trans. Microwave Theory Tech.*, vol. 56, no. 7, pp. 1721-1728, 2008.

[2] S. Zheng, W. S. Chan, S. H. Leung, and Q. Xue, "Broadband Butler matrix with flat coupling," *Electronics Lett.*, vol. 43, no. 10, pp. 576-577, 2007.

[3] S.Y. Zheng, W.S. Chan and Y.S. Wong, "Reconfigurable RF quadrature patch hybrid coupler," *IEEE Trans. Industrial Electr.*, vol. 60, no. 8, pp. 3349-3359, 2013.

[4] S.Y. Zheng, J.H. Deng, Y.M. Pan and W.S. Chan, "Circular sector patch hybrid coupler with an arbitrary coupling coefficient and phase difference," *IEEE Trans. Microwave Theory Tech.*, vol. 61, no. 5, pp. 1781-1792, 2013.

[5] S.Y. Zheng, S.H. Yeung, W.S. Chan, K.F. Man, and S.H. Leung, "Size-reduced rectangular patch hybrid coupler using patterned ground plane," *IEEE Trans. Microwave Theory Tech.*, vol. 57, no. 1, pp. 180-188, 2009.

[6] S. Sun and L. Zhu, "Miniaturised patch hybrid couplers using asymmetrically loaded cross slots," *IET Microwaves, Ant. Prop.*, vol. 4, no. 9, pp. 1427-1433, 2010.

[7] X.F. Ye, S.Y. Zheng, and Y.M. Pan, "A compact millimeter-wave patch quadrature coupler with a wide range of coupling coefficients," *IEEE Microwave Wireless Comp. Lett.*, vol. 26, no. 3, pp. 165-167, 2016.

[8] T. Kawai and I. Ohta, "Planar-circuit-type 3-dB quadrature hybrids," *IEEE Trans. Microwave Theory Tech.*, vol. 42, no. 12, pp. 2462-2467, 1994.

[9] M. Ghassemi, M. Bakr, and N. Sangary, "Antenna design exploiting adjoint sensitivity-based geometry evolution," *IET Microwaves, Ant. Prop.*, vol. 7, no. 4, pp. 268-276, 2013.

[10] M. John and M.J. Ammann, "Antenna optimization with a computationally efficient multiobjective evolutionary algorithm," *IEEE Trans. Ant. Prop.*, vol. 57, no. 1, pp. 260-263, 2007.

[11] CST Microwave Studio, ver. 2013, Dassault Systems, 10 rue Marcel Dassault, CS 40501, Vélizy-Villacoublay Cedex, France, 2013.

[12] S. Koziel and A. Bekasiewicz, "Expedited simulation-driven design optimization of UWB antennas by means of response features," *Int. J. RF Microwave CAE*, vol. 27, no. 6, pp. 1-8, 2017.

[13] A.R. Conn, N.I.M. Gould, and P.L. Toint, *Trust Region Methods*, MPS-SIAM Series on Optimization, 2000.

[14] A. Akdagli, "A novel expression for effective radius in calculating the resonant frequency of circular microstrip patch antennas," *Microwave, Opt. Technol. Lett.*, vol. 49, no. 10, pp. 2395-2398, 2007.